ORIGINAL RESEARCH ARTICLE

Integrated Experimental and Thermodynamic Modeling Study of the Pb-Fe-O-S-Si System: Effect of Temperature and $p(SO_2)$ on Slag-Matte-Metal-Tridymite Equilibria

T. HIDAYAT, A. FALLAH-MEHRJARDI, H. ABDEYAZDAN, D. SHISHIN, M. SHEVCHENKO, P.C. HAYES, and E. JAK

An integrated experimental and thermodynamic modeling study has been used to characterize phase equilibria in the Pb-Fe-O-S-Si system. The experimental approach developed for investigation of this system, which involves the use of high-temperature equilibration, quenching, and electron probe X-ray microanalysis, has enabled to overcome difficulties associated with high corrosive tendency of the condensed phases and high vaporization rates of Pb species specific to this system. The study shows that systematic, accurate direct experimental measurements of the Pb, Fe, Si, and S concentrations in the coexisting phases in this system are now possible. The results obtained for the slag-matte-metal-tridymite phase equilibria at 1100 °C and 1200 °C appear to be the first systematic quantitative experimental data on phase compositions in equilibrium in the Pb-Fe-O-S-Si system. First systematic experimental measurements have also been undertaken for the gas-slag-matte-tridymite equilibria at $p(SO_2)$ = 0.6 atm at 1200 °C. Thermodynamic calculations have been performed using the FactSage thermodynamic package. The experimental data have been used, along with other relevant measurements, to develop a self-consistent thermodynamic database that can be used for optimization of industrial processes.

https://doi.org/10.1007/s11663-022-02707-y

I. INTRODUCTION

CHARACTERIZATION of phase equilibria and thermodynamics of the Pb-Fe-O-S-Si multi-phase gas-slag-matte-metal-solid oxide chemical system—the focus of the present study—is important since this system forms the basis for the industrial pyrometallurgical processing of complex lead-containing primary and secondary materials.

In primary lead smelting, the conditions of matte formation have to be controlled to prevent the formation of sulfide accretions, as in KIVSET furnace.[1] The matte phase appears at reducing conditions in the lead blast furnace processes.[2] In the secondary lead smelting, the matte phase is used to remove sulfur from battery materials.[3] The formation of matte can be targeted as a part of integrated polymetallic process.[4] Mattes in many processes[2,4] are enriched in copper, slags typically contain Zn, Fe, Ca, and Si oxides. The distribution of minor elements is important in these processes.

Obtaining accurate experimental measurements in this system under controlled process conditions is particularly difficult for several reasons. Liquid lead metal, matte, and slag phases are all excellent solvents, and readily react with and dissolve refractory metals and oxides—this highly corrosive behavior is one of the experimental difficulties. In addition, high vapor pressures of lead metal, sulfide, and oxide species at high temperatures and conditions of interest to industrial processes result in rapid vaporization of lead-containing species in open systems.

T. HIDAYA is with the Pyrometallurgy Innovation Centre (PYROSEARCH), School of Chemical Engineering, The University of Queensland, Brisbane, QLD 4072, Australia and also with the Metallurgical Engineering Department, Bandung Institute of Technology, Bandung, West Java 40132, Indonesia. A. FALLAH-MEHRJARDI is with the Vesuvius, Rue de Douvrain 17, 7011 Mons, Belgium. H. ABDEYAZDAN, D. SHISHIN, M. SHEVCHENKO, P.C. HAYES, and E. JAK1 are with the Pyrometallurgy Innovation Centre (PYROSEARCH), School of Chemical Engineering, The University of Queensland. Contact e-mail: h.abdeyazdan@uq.edu.au

Manuscript submitted April 12, 2022; accepted December 9, 2022.
Article published online January 23, 2023.

For these reasons, there is little information available in the literature on this system. Rytkonen and Taskinen[5] studied the distribution of impurities between lead metal and lead silicate slag, including conditions in SO_2 atmosphere, but the matte phase was not present in the experiment. Fontainas *et al.*[6] provided the relationship between the Pb concentration in slag and the PbS:Cu_2S:(FeS + ZnS) ratio in mattes in the range of conditions limited to 1.0–3.5 wt pct Pb in slag and mattes rich in copper. Amout *et al.*[7] conducted thermodynamic calculations for the Pb-Fe-O-S-Si system at 1200 °C and showed the conditions of slag-matte-metal equilibrium on the Yazawa-like diagram $p(O_2)$ vs $p(S_2)$, but this work was theoretical, no experiments were conducted. Experimental and modeling work is available in a number of sources for the slag-matte-Fe(fcc) equilibria in the Fe-O-S-Si sub-system.[8–11] The concentration of sulfur in slag for the slag-solid PbS-Pb metal equilibrium in the Pb-O-S-Si sub-system has been recently studied and modeled.[12] Experimental work data for the Pb-Fe-S sub-system are available.[13–21] It was thermodynamically assessed by Decterov and Pelton,[22] and later by Johto and Taskinen.[20] These previous results were used in the present study to develop the model for the liquid matte/metal solution. No systematic quantitative experimental data on the phases in equilibrium in the Pb-Fe-O-S-Si system were found in literature.

The present study reports phase equilibrium results, obtained for the first time through the high-temperature equilibration, rapid quenching technique, and electron probe X-ray microanalysis of the equilibrated phases for the slag-matte-metal-tridymite in the closed Pb-Fe-O-S-Si system at 1100 °C and 1200 °C, as well as results for the open gas-slag-matte-tridymite system at 1200 °C and fixed $p(SO_2)$ of 0.6 atm. The compositions of phases measured experimentally were compared and critically assessed using thermodynamic calculations by FactSage software.

II. RESEARCH METHODOLOGY

A. *Experimental Technique*

The experimental technique used in the present study is based on the general approach involving high-temperature equilibration, quenching, and direct measurement of the compositions of phases in chemical equilibrium using electron probe X-ray microanalysis outlined in the previous publications by the authors.[23,24] The development of the experimental technique specific to this chemical system has been described in a recent paper by the authors.[25]

Synthetic samples used in the present study were prepared from mixtures of high-purity (99.9 pct) metals (Fe, Pb), sulfides (PbS, FeS), elemental sulfur and oxides (Fe_2O_3, PbO, SiO_2) powders supplied by Alfa Aesar, MA. Separate master slags and master mattes of selected compositions were prepared. The PbO-SiO_2 (60 mol. pct SiO_2) master slag was obtained by melting a mixture of Pb_3O_4 and pre-dried SiO_2 powders in platinum crucible at 800–900 °C for 1 h; Pb_3O_4 was made by oxidation of PbO in air for 1 day at 450 °C in an MgO crucible. Higher oxidation of Pb was needed to protect Pt crucibles from possible damage due to the formation of the Pb-Pt liquid in case when conditions were not sufficiently oxidizing. The formation of Pb_3O_4 is expected under these conditions according to the phase diagram of the PbO system,[26] but was not verified by XRD or other method, since the only purpose of oxidation of PbO was to protect the Pt crucibles, and that purpose was achieved. The FeO-Fe_2O_3-SiO_2 master slag was prepared by melting a mixture of Fe, Fe_2O_3, and pre-dried SiO_2 powders in the pure SiO_2 glass ampoule at 1250–1300 °C in an argon atmosphere; after preparation the slag was physically separated from the silica ampoule. The PbS-FeS-Pb master matte or metal was prepared by slowly heating the mixture of Pb, S, and FeS powders in graphite crucibles or silica ampoules for several hours at temperatures up to 1000 °C in an argon atmosphere. The commercially available sulfide powders were found to oxidize during the storage, so the preparation of master matte or metal was necessary to ensure that oxygen-free material was used in the experiments. The precursor materials were pulverized, mixed to the desired bulk compositions and pelletized; 0.5 g samples were introduced into silica ampoules (13 mm ID, 1 mm wall thickness). Two experimental setups were used: closed system and semi-open system. Closed system experiments are suitable for the slag-matte-metal-tridymite equilibria at fixed temperature and total pressure of 1 atm, corresponding to the lowest possible $p(SO_2)$ in the system. According to the Gibbs phase rule, all degrees of freedom are fixed. The $p(O_2)$ in the system is established from initial mixture, but not measured. For the slag-matte equilibria, one more degree of freedom must be fixed, which is the $p(SO_2)$ in the system. It is possible to fix the $p(SO_2)$ by the flow of gas. Thus, the slag-matte equilibria experiments require semi-open experimental setup. In this setup, the $p(O_2)$ is established by the gas flow, not from the initial mixture.

i. Closed system experiments: silica ampoules were evacuated to < 0.01 atm pressure, filled with and sealed using an oxyhydrogen burner
ii. Semi-open experimental setup: silica wool was placed in the middle part of the ampoule, which was then sealed at atmospheric pressure. Next, a small orifice (2–3 mm diameter) was made in the upper portion of the ampoule (Figure 1). The samples were equilibrated in the flow pf $CO/CO_2/SO_2/Ar$ atmospheres For example, the target atmosphere of $p(SO_2) = 0.6$ atm and $p(O_2) = 10^{-8}$ atm at 1200 °C was obtained using the gas mixture of 2.87 vol. pct CO (20 pct CO in argon), 29.87 vol. pct CO_2, and 68.26 vol. pct SO_2 with a flow rate of 400–500 ml/min. Gas volumes were calculated using FactSage FactPS database. The selected $p(SO_2) = 0.6$ atm is the highest that still allows enough volume for CO and CO_2 to effectively control the $p(O_2)$. Higher values of $p(SO_2)$ increase the reaction rates and ensure conditions further from equilibrium with metal (low $p(SO_2)$), so

that a wider range of conditions is covered. The oxygen partial pressure was periodically tested in the furnace output gas, but only for the sulfur-free gas mixture (CO_2-CO-Ar). It was in agreement with the calculations. The sulfur in gas would damage the sensor, therefore no $p(O_2)$ measurements were possible for the SO_2-CO_2-CO-Ar gases.

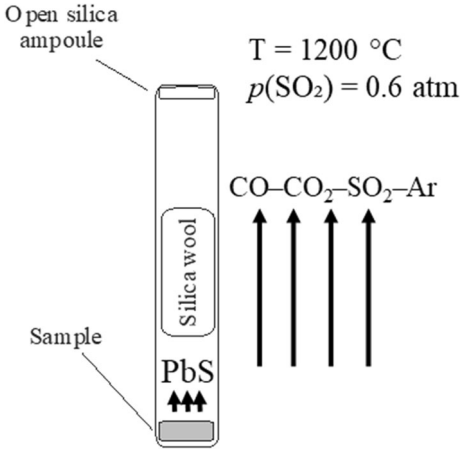

Fig. 1—Schematic of a semi-open silica ampoule used for equilibration at fixed $p(SO_2) = 0.6$ atm.

The ampoules were heated to the equilibration temperature in the uniform hot zone in a vertical electrically heated resistance furnace. The flowing gas atmospheres were passed over the ampoules, which were suspended within an impervious alumina reaction tube.

After the designated equilibration time, the samples were quenched rapidly in the $CaCl_2$ brine at − 20 °C, washed, dried, mounted in epoxy resin, polished, and the equilibrium phase compositions were measured by the electron probe X-ray microanalyzer (EPMA, JEOL JXA 8200L, trademark of Japan Electron Optics Ltd., Tokyo) using an acceleration voltage of 15 keV and a probe current of 20 nA. The Duncumb–Philibert ZAF correction procedure supplied with the JEOL JXA 8200L probe was applied. SiO_2, Fe_2O_3, Fe, FeS_2, PbS reference materials from Charles M. Taylor, Stanford, CA, and the PbO-SiO_2 K456 glass (71.4 wt pct PbO) from NIST, Gaithersburg, MD, were used as standards. EPMA measurements with beam diameters between 10 and 50 μm were undertaken to obtain representative compositions of the phases for cases in which partial crystallization occurred on quenching. As demonstrated previously,[27] for these particular measurements, increasing the probe diameter was found to decrease the uncertainty of the phase composition measurements. Iron is always present in slag in the Fe^{2+} and Fe^{3+} forms. Only concentrations of the metal cations in the

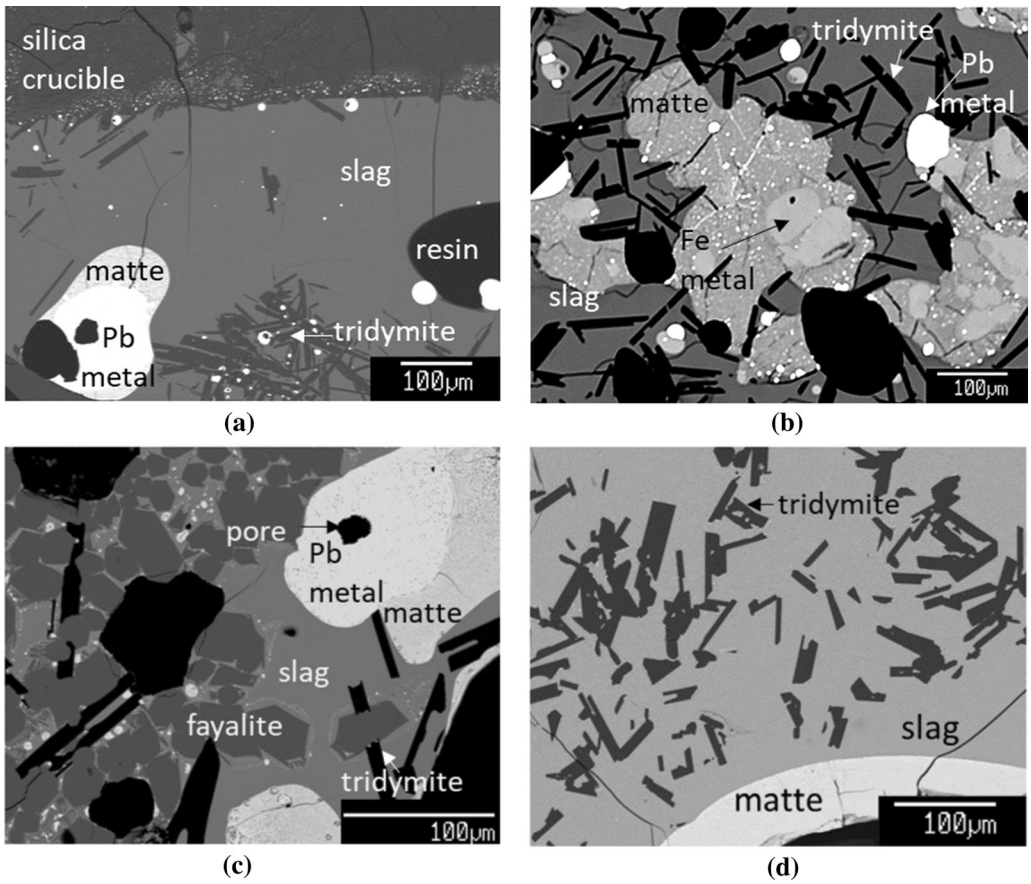

Fig. 2—Examples of microstructures of quenched samples in the Pb-Fe-O-S-Si system for the (*a*) slag-matte-Pb metal-tridymite equilibria at 1200 °C, (*b*) slag-matte-Pb metal-Fe metal-tridymite equilibria at 1200 °C, (*c*) slag-matte-Pb metal-fayalite-tridymite equilibria at 1100 °C, and (*d*) gas-slag-matte-tridymite equilibria at 1200 °C and $p(SO_2) = 0.6$ atm.

Table I. Measured Phase Compositions for the Closed System, Slag-Matte-Pb Metal-Tridymite for Pb-Fe-O-S-Si at 1200 °C

		Elemental composition (wt pct)						Oxide composition (wt pct)					
No	Phase	Pb	Fe	S	Si	O	Phase	PbO	FeO	S	SiO_2	Fe/SiO_2 in slag	Pb in slag
1	matte	82.1 ± 0.6	3.9 ± 0.5	14.0 ± 0.2	0.01 ± 0.01	n/a	slag	40.7 ± 0.7	28.1 ± 0.4	1.10 ± 0.2	30.0 ± 0.6	0.73	37.8
	Pb metal	92.7 ± 1.2	0.7 ± 0.2	6.6 ± 1.0	0.00	n/a	tridymite				> 99		
2	matte	74.0 ± 0.5	10.2 ± 0.4	15.8 ± 0.1	0.00	n/a	slag	35.0 ± 0.3	35.1 ± 0.2	2.3 ± 0.1	27.6 ± 0.2	0.99	32.5
	Pb Metal	not measured					tridymite				> 99		
3	matte	74.1 ± 1.5	10.1 ± 1.3	15.8 ± 0.3	0.00	n/a	Slag	32.9 ± 0.2	36.3 ± 0.2	2.1 ± 0.04	28.8 ± 0.2	0.98	30.5
	Pb metal	not measured					tridymite				> 99		
4	matte	64.0 ± 0.7	18.1 ± 0.5	17.8 ± 0.2	0.08 ± 0.03	n/a	slag	21.6 ± 0.7	47.7 ± 0.5	2.6 ± 0.2	28.2 ± 0.6	1.32	20.1
	Pb metal	97.9 ± 0.4	0.05 ± 0.03	2.1 ± 0.4	0.00	n/a	tridymite				> 99		
5	matte	65.2 ± 0.8	17.1 ± 0.6	17.6 ± 0.2	0.05 ± 0.03	n/a	slag	20.3 ± 0.2	48.9 ± 0.2	2.7 ± 0.05	28.1 ± 0.2	1.35	18.9
	Pb metal	98.5 ± 1.1	0.3 ± 0.2	1.25 ± 1.1	0.00	n/a	tridymite				> 99		
6	matte	62.4 ± 0.7	18.0 ± 0.5	17.3 ± 0.3	0.00	2.4 ± 0.2	slag	25.7 ± 0.2	44.6 ± 0.3	3.6 ± 0.07	26.1 ± 0.2	1.33	23.9
	Pb metal	96.7 ± 0.2	0.43 ± 0.1	2.92 ± 0.1	0.00	n/a	tridymite				> 99		
7	matte	60.2 ± 1.0	21.0 ± 0.9	18.7 ± 0.9	0.12 ± 0.1	n/a	slag	20.3 ± 0.9	50.2 ± 0.8	4.4 ± 0.1	25.1 ± 0.8	1.55	18.9
	Pb metal	98.7 ± 0.2	0.25 ± 0.1	1.07 ± 0.2	0.00	n/a	tridymite				> 99		
8	matte	60.2 ± 1.0	20.6 ± 0.8	19.2 ± 0.2	0.00	n/a	slag	19.3 ± 0.6	51.4 ± 0.3	4.4 ± 0.2	24.9 ± 0.6	1.61	17.9
	Pb metal	98.8 ± 0.3	0.08 ± 0.07	1.16 ± 0.3	0.00	n/a	tridymite				> 99		
9	matte	48.8 ± 0.4	30.8 ± 0.3	20.2 ± 0.3	0.19 ± 0.02	n/a	slag	17.4 ± 0.3	54.1 ± 0.2	4.6 ± 0.07	23.8 ± 0.4	1.77	16.2
	Pb metal	97.9 ± 0.8	0.39 ± 0.3	1.69 ± 0.5	0.00	n/a	tridymite				> 99		
10	matte	24.7 ± 1.2	47.1 ± 0.8	22.1 ± 0.2	0.40 ± 0.04	5.7 ± 0.2	slag	10.8 ± 0.2	60.4 ± 0.3	6.7 ± 0.06	22.1 ± 0.2	2.12	10.0
	Pb metal	98.4 ± 0.4	0.37 ± 0.1	1.19 ± 0.3	0.00	n/a	tridymite				> 99		
11	matte	21.6 ± 1.5	52.0 ± 1.1	25.9 ± 0.4	0.52 ± 0.05	n/a	slag	8.7 ± 0.2	61.5 ± 0.2	6.4 ± 0.08	23.4 ± 0.2	2.04	8.1
	Pb metal	not measured					tridymite				> 99		
12	matte	9.6 ± 2.9	62.8 ± 2.5	27.2 ± 0.7	0.45 ± 0.03	n/a	slag	5.4 ± 0.2	64.5 ± 0.2	6.6 ± 0.07	23.5 ± 0.2	2.13	5.0
	Pb metal	99.4 ± 0.3	0.19 ± 0.08	0.43 ± 0.3	0.00	n/a	tridymite				> 99		
13	matte	8.0 ± 1.9	59.7 ± 1.3	25.2 ± 0.5	0.35 ± 0.04	6.8 ± 0.3	slag	4.5 ± 0.1	66.1 ± 0.1	6.9 ± 0.05	22.6 ± 0.2	2.27	4.1
	Pb metal	99.3 ± 0.2	0.25 ± 0.09	0.47 ± 0.2	0.00	n/a	tridymite				> 99		
14	matte	6.8 ± 1.9	60.4 ± 1.4	26.3 ± 0.5	0.26 ± 0.05	6.2 ± 0.2	slag	4.7 ± 0.2	64.9 ± 0.2	6.5 ± 0.05	23.9 ± 0.1	2.11	4.4
	Pb metal	99.2 ± 0.4	0.37 ± 0.2	0.41 ± 0.3	0.00	n/a	tridymite				> 99		
15	matte	5.6 ± 1.5	61.1 ± 1.1	27.3 ± 0.7	0.09 ± 0.03	5.9 ± 0.6	slag	3.7 ± 0.1	65.8 ± 0.2	5.9 ± 0.05	24.6 ± 0.2	2.08	3.4
	Pb metal	99.5 ± 0.2	0.31 ± 0.1	0.22 ± 0.1	0.00	n/a	tridymite				> 99		
16	matte	4.3 ± 1.8	66.5 ± 1.9	29.2 ± 1.7	0.04 ± 0.03	n/a	slag	1.70 ± 0.2	66.7 ± 0.4	4.5 ± 0.07	27.2 ± 0.4	1.91	1.58
	Pb metal	99.9 ± 0.1	0.10 ± 0.1	0.00	0.00	n/a	tridymite				> 99		
	Fe metal	< 0.1	99.9 ± 0.1	0.04 ± 0.01	0.02 ± 0.02	n/a							
17	matte	3.8 ± 0.9	66.1 ± 0.8	30.1 ± 1.0	0.02 ± 0.02	n/a	slag	1.84 ± 0.1	66.6 ± 0.2	4.5 ± 0.06	27.1 ± 0.1	1.91	1.71
	Pb metal	99.83 ± 0.1	0.17 ± 0.1	0.00	0.00	n/a	tridymite				> 99		
	Fe metal	< 0.06	99.9 ± 0.1	0.04 ± 0.01	0.00	n/a							
18	matte	4.8 ± 0.3	63.6 ± 1.7	27.7 ± 1.4	0.00	3.9	slag	1.43 ± 0.1	66.1 ± 0.1	4.7 ± 0.05	27.7 ± 0.1	1.85	1.33
	Pb metal	99.61 ± 0.1	0.29 ± 0.04	0.11 ± 0.04	0.00	n/a	tridymite				> 99		
	Fe metal	0.04 ± 0.04	99.7 ± 0.1	0.02 ± 0.01	0.00	0.26							

Table II. Measured Phase Compositions for the Closed System, Slag-Matte-Pb Metal-Tridymite for Pb-Fe-O-S-Si at 1100 °C

		Elemental composition (wt pct)					Oxide composition (wt pct)					
No	Phase	Pb	Fe	S	Si	Phase	PbO	FeO	S	SiO_2	Fe/SiO_2 in slag	Pb in slag
1	matte	82.6 ± 1.0	3.8 ± 0.6	13.6 ± 0.6	0.00	slag	41.3 ± 0.7	28.8 ± 0.4	0.33 ± 0.1	29.5 ± 1.1	0.76	38.4
	Pb metal	95.1 ± 1.4	0.25 ± 0.2	4.6 ± 1.3	0.00	tridymite				> 99		
2	matte	77.0 ± 1.6	7.7 ± 1.3	15.3 ± 0.3	0.00	slag	35.2 ± 0.4	35.1 ± 0.8	1.94 ± 0.1	27.7 ± 0.5	0.98	32.7
	Pb metal	95.0 ± 2.4	0.48 ± 0.4	4.5 ± 2.0	0.00	tridymite				> 99		
3	matte	76.0 ± 0.9	8.7 ± 0.8	15.2 ± 0.2	0.00	slag	34.5 ± 0.3	36.6 ± 0.2	1.82 ± 0.1	27.1 ± 0.1	1.05	32.0
	Pb metal	Not measured				tridymite				> 99		
4	matte	78.6 ± 2.0	6.8 ± 1.4	14.6 ± 0.8	0.00	slag	34.5 ± 0.3	35.5 ± 0.3	1.59 ± 0.03	28.4 ± 0.1	0.97	32.0
	Pb metal	96.6 ± 1.0	0.18 ± 0.1	3.3 ± 0.9	0.00	tridymite				> 99		
5	matte	71.8 ± 0.3	11.6 ± 0.2	16.6 ± 0.1	0.00	slag	29.1 ± 0.4	40.5 ± 0.4	2.5 ± 0.1	27.9 ± 0.4	1.13	27.0
	Pb metal	97.1 ± 0.3	0.18 ± 0.1	2.6 ± 0.2	0.08 ± 0.06	tridymite				> 99		
6	matte	70.8 ± 1.1	12.7 ± 0.9	16.6 ± 0.3	0.00	slag	28.5 ± 0.4	42.3 ± 0.5	2.7 ± 0.1	26.5 ± 0.2	1.24	26.4
	Pb metal	97.4 ± 1.0	0.11 ± 0.1	2.5 ± 0.9	0.02 ± 0.02	tridymite				> 99		
7	matte	71.7 ± 5.0	12.2 ± 4.0	16.1 ± 1.0	0.01 ± 0.01	slag	25.5 ± 0.4	45.1 ± 0.4	2.7 ± 0.1	26.7 ± 0.5	1.32	23.6
	Pb metal	97.9 ± 1.6	0.10 ± 0.1	1.94 ± 1.6	0.01 ± 0.01	tridymite				> 99		
8	matte	66.1 ± 1.2	16.4 ± 0.8	17.4 ± 0.5	0.01 ± 0.01	slag	24.0 ± 0.9	46.9 ± 0.9	3.2 ± 0.1	26.0 ± 0.2	1.40	22.2
	Pb metal	97.3 ± 0.6	0.23 ± 0.2	2.5 ± 0.5	0.00	tridymite				> 99		
9	matte	60.8 ± 0.7	21.0 ± 0.5	18.0 ± 0.2	0.09 ± 0.09	slag	21.5 ± 0.3	50.0 ± 0.4	3.7 ± 0.05	24.7 ± 0.4	1.57	20.0
	Pb metal	97.8 ± 1.0	0.3 ± 0.3	1.94 ± 0.6	0.06 ± 0.6	tridymite				> 99		
						fayalite	< 0.08	70.9 ± 0.1	0.00	29.0 ± 0.1		

Table III. Measured Phase Compositions for the Semi-Open System, Gas-Slag-Matte-Tridymite for Pb-Fe-O-S-Si at 1200 °C and $p(SO_2) = 0.6$ atm

		Matte composition (wt pct)					Oxide composition (wt pct)					
No	Equilib. time, hour	Pb	Fe	S	Si	Phase	PbO	FeO	S	SiO_2	Fe/SiO_2 in slag	Pb in slag
1	3	69.6 ± 3	13.3 ± 2	16.1 ± 1	0.05	slag	42.1 ± 2.0	27.5 ± 1.4	1.68 ± 0.6	28.7 ± 1.6	0.75	39.1
						tridymite				> 99		
2	3	76.9 ± 2	8.0 ± 1	14.9 ± 1	0.20 ± 0.1	slag	41.6 ± 2.0	29.1 ± 1.5	2.2 ± 0.6	27.2 ± 2.0	0.83	38.6
						tridymite				> 99		
3	0.5	75.9 ± 3	8.8 ± 2	15.2 ± 1	0.03	slag	41.5 ± 1	29.0 ± 1	2.0 ± 0.5	27.4 ± 1	0.82	38.6
						tridymite				> 99		
4	3	72.6 ± 3	11.3 ± 2	16.0 ± 1	0.02	slag	36.2 ± 0.4	35.0 ± 0.3	2.7 ± 0.2	26.1 ± 0.2	1.04	33.6
						tridymite				> 99		
5	0.5	71.1 ± 3	13.0 ± 2	15.8 ± 1	0.10 ± 0.1	slag	35.4 ± 0.5	36.0 ± 0.4	2.7 ± 0.2	25.9 ± 0.3	1.08	32.9
						tridymite				> 99		
6	3	66.3 ± 2	17.3 ± 1	16.2 ± 1	0.19 ± 0.1	slag	33.9 ± 0.5	38.4 ± 0.5	3.6 ± 0.2	24.1 ± 0.2	1.24	31.5
						tridymite				> 99		
7	3	69.1 ± 1	14.4 ± 1	16.4 ± 0.5	0.13 ± 0.1	slag	33.5 ± 0.5	37.8 ± 0.5	2.9 ± 0.2	25.8 ± 0.2	1.14	31.1
						tridymite				> 99		
8	3	67.6 ± 2	15.7 ± 1	16.5 ± 0.5	0.16 ± 0.1	slag	30.9 ± 0.6	39.5 ± 0.5	2.7 ± 0.2	26.9 ± 0.2	1.14	28.7
						tridymite				> 99		
9	0.5	61.4 ± 2	21.0 ± 2	17.1 ± 0.3	0.35 ± 0.1	slag	30.5 ± 0.7	42.5 ± 0.5	4.2 ± 0.2	22.8 ± 0.4	1.45	28.3
						tridymite				> 99		
10	3	58.1 ± 1	23.8 ± 1	17.6 ± 0.3	0.48 ± 0.1	slag	29.5 ± 0.2	43.7 ± 0.2	4.6 ± 0.1	22.3 ± 0.1	1.53	27.3
						tridymite				> 99		
11	5	57.7 ± 1	24.1 ± 1	17.6 ± 0.3	0.47 ± 0.1	slag	29.0 ± 0.5	44.4 ± 0.4	4.9 ± 0.2	21.7 ± 0.2	1.59	26.9
						tridymite				> 99		

Table IV. Model Parameters for Solution Phases Used for Thermodynamic Calculations of the Present Study

	Reference or Model Parameter, J mol^{-1}
Slag	$(Pb^{2+}, Fe^{2+}, Fe^{3+}, Si^{4+})(O^{2-}, S^{2-})$, MQMQA Refs. [34–36]
Pb-Fe-O-Si sub-system	Ref. [37]
Fe-O-S-Si sub-system	Refs. [10, 35, 38]
Pb-Si-O-S sub-system	$Z(Pb^{2+}) = Z(S^{2-}) = 1.37744$, $\zeta_{Pb^{2+}S^{2-}}$ 1.377
g°_{PbS}	$-79{,}525.2842 + 367.3552\ T - 69.0360 T \ln T$
$g^{001}_{Si^{4+}Pb^{2+}/O^{2-}O^{2-}(S^{2-})}$	16,736
$g^{10}_{Fe^{2+}Pb^{2+}/S^{2-}S^{2-}}$ (Bragg–Williams)	12,552
$g^{10}_{Fe^{3+}Pb^{2+}/S^{2-}S^{2-}}$ (Bragg–Williams)	12,552
Matte/metal	$(Fe^{II}, Fe^{III}, Pb^{II}, O^{II}, S^{II})$, MQMPA Refs. [38–45]
Fe-O-S	Ref. [44]
Pb-S	[46]
Fe-Pb	Refs. [47, 48]
Pb-Fe-S	
$g^{001}_{Fe^{II}S^{II}(Pb^{II})}$	$-13{,}807.2$
$g^{001}_{Fe^{II}Pb^{II}(S^{II})}$	$-37{,}656.0$
$g^{202}_{Pb^{II}S^{II}(Fe^{II})}$	$-50{,}208.0$
Pb-O	$Z^{Pb^{II}}_{Pb^{II}O^{II}} = Z^{O^{II}}_{Pb^{II}O^{II}} = 2$
$\Delta g^{\circ}_{Pb^{I}O^{II}}$	$-335{,}975.2 + 80.83488\ T - 8.368 T \ln T$
$g^{10}_{Pb^{II}O^{II}}$	$175{,}728.0 - 75.312\ T$
$g^{30}_{Pb^{II}O^{II}}$	$-105{,}855.2 + 54.3920\ T$
$g^{01}_{Pb^{II}O^{II}}$	41,840.0
Metallic Fe (fcc)	(Fe, O, S), BW Refs. [38, 42, 43]
Tridymite (SiO_2) (stoichiometric compound)	Ref. [49]

MQMQA modified quasichemical model in quadruplet approximation, *MQMPA* modified quasichemical model in pair approximation, *BW* Bragg–Williams model.

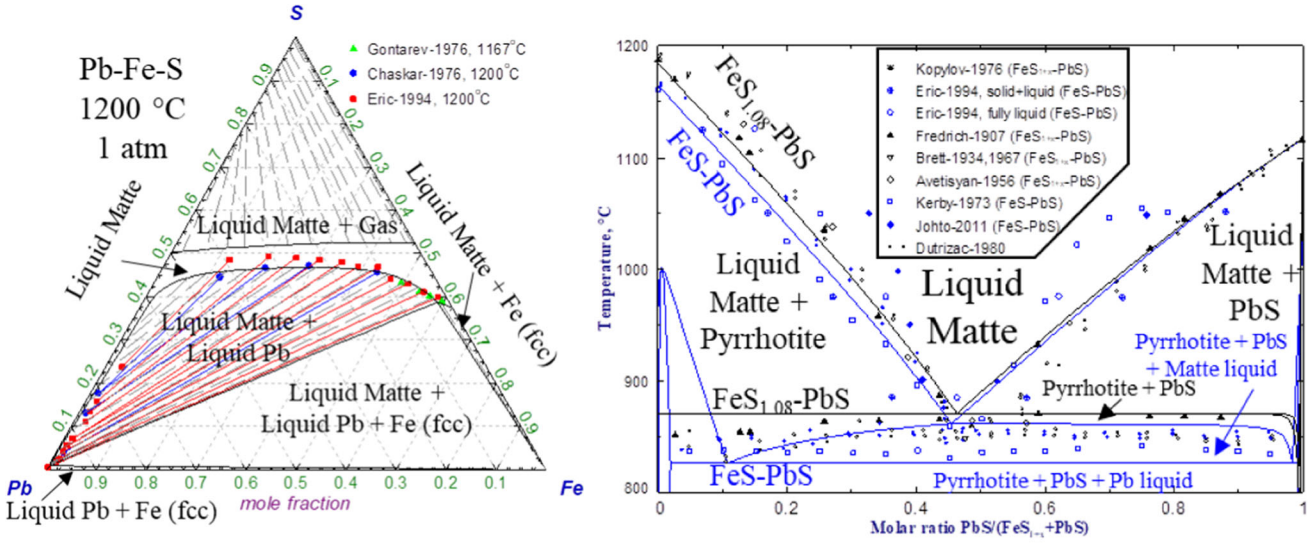

(a) **(b)**

Fig. 3—Thermodynamic model predictions for the Pb-Fe-S system: (*a*) phase diagram at 1200 °C compared to literature data.[13–15] (*b*) Pseudo-binary sections; blue line FeS-PbS,[14,16,20,21] black line—$FeS_{1.08}$-PbS.[17–19,21] (Color figure online).

slag were measured with EPMA in the present study. The compositions of the phases were recalculated to select oxidation states for presentation purposes and to unambiguously report compositions. Oxygen in matte was measured directly in selected samples only using LDE1 crystal and Fe_3O_4 standard. The technique was similar to described by Sineva *et al.*[28] for the Cu-Fe-Si-O-S system.

It has been shown in previous studies[29–31] that for the high-lead slag systems the standard JEOL ZAF correction results in significant uncertainties in absolute concentrations of the components. The values of the compositions of the stoichiometric solids after only standard JEOL ZAF correction were systematically deviating from actual values by up to 1 mol. pct. For this reason, the EPMA measurements after the standard JEOL ZAF correction were further adjusted using a custom-developed approach based on using secondary standards made of stoichiometric solids (Fe_2SiO_4, $PbSiO_3$, Pb_2SiO_4). The correction involved converting the composition of the slag molar fraction. Then the composition was normalized to exclude sulfur. Correction formulas for the sulfur-free slag phase taken from[29] were then applied:

$$x_{SiO_2}^{corrected} = x_{SiO_2} - x_{SiO_2}x_{PbO}\left(-0.0129 - 0.0206x_{SiO_2} + 0.421x_{SiO_2}^2 - 0.4066x_{SiO_2}^3\right) - 0.0637x_{FeO}x_{SiO_2}(1 - x_{SiO_2}) \quad [1]$$

$$x_{PbO}^{corrected} = x_{PbO}\frac{1 - x_{SiO_2}^{corrected}}{1 - x_{SiO_2}}, \quad [2]$$

$$x_{FeO}^{corrected} = x_{FeO}\frac{1 - x_{SiO_2}^{corrected}}{1 - x_{SiO_2}}, \quad [3]$$

where x_{PbO}, x_{FeO} , and x_{SiO_2} are initial values after only a standard JEOL ZAF correction. Finally, sulfur was added back and composition normalized again to 100 pct total.

B. *Thermodynamic Modeling*

Thermodynamic calculations and development of solutions models for the phases were carried out using the FactSage 7.3 thermodynamic package with an internal database. The Modified Quasichemical Model in Quadruplet Approximation (MQMQA) was used for the slag phase, Modified Quasichemical Model in Pair Approximation (MQMPA) was used to describe the thermodynamic behavior of the liquid matte and metal phases. Details of the thermodynamic models, and optimization of model parameters for the liquid slag, matte, and metal phases have been discussed earlier.[23,24,32,33] Few model parameters have been introduced or updated in course of the present study, as will be discussed in Section III–B.

III. RESULTS

A. *Experimental Results*

The results of two series of experiments are reported in the present paper for the Pb-Fe-O-S-Si system:

- Closed system, slag-matte-Pb metal-tridymite at 1100 °C and 1200 °C,
- Semi-open system, gas-slag-matte-tridymite at 1200 °C and $p(SO_2) = 0.6$ atm.

Examples of typical microstructures obtained in these experimental series are presented in Figures 2(a) through (d). The normalized compositions of the phases measured by the EPMA are given in Tables I, II, and III. Since the experiments were undertaken in equilibrium with tridymite, this phase is present in all samples. Figure 2(a) shows the remains of the ampoule, but in addition to that platy secondary tridymite crystals were observed in the slag phase, indicating that equilibrium with tridymite was achieved. Due to surface tension, the matte phase is located in close contact with the liquid Pb metal (Figures 2(a) through (c)) and solid iron metal (Figure 2(b)) phases when the latter is present. Large droplets of Pb (20–100 μm diameter) observed in the slag are metallic phase existing in equilibrium with slag at high temperature. Fine droplets of Pb with the diameters of less than 5 μm are observed in the matte phase. These are believed to have formed during the quenching process and do not represent equilibrium at high temperature. Faceted crystals of the fayalite (Fe_2SiO_4) phase can be seen in Figure 2(c).

B. *Thermodynamic Modeling Results*

Most thermodynamic model parameters were adopted from the earlier studies without modifications. The references for the corresponding sub-systems are provided in Table IV. The values of parameters that have not been published before are also listed in Table IV. The values for $g^{001}_{Fe^{II}S^{II}(Pb^{II})}$, $g^{001}_{Fe^{II}Pb^{II}(S^{II})}$, and $g^{202}_{Pb^{II}S^{II}(Fe^{II})}$ were optimized to describe available experimental data in the Pb-Fe-S reviewed by Decterov and Pelton.[22] Selected results are demonstrated in Figure 3. The modeling results by more recent study by Johto and

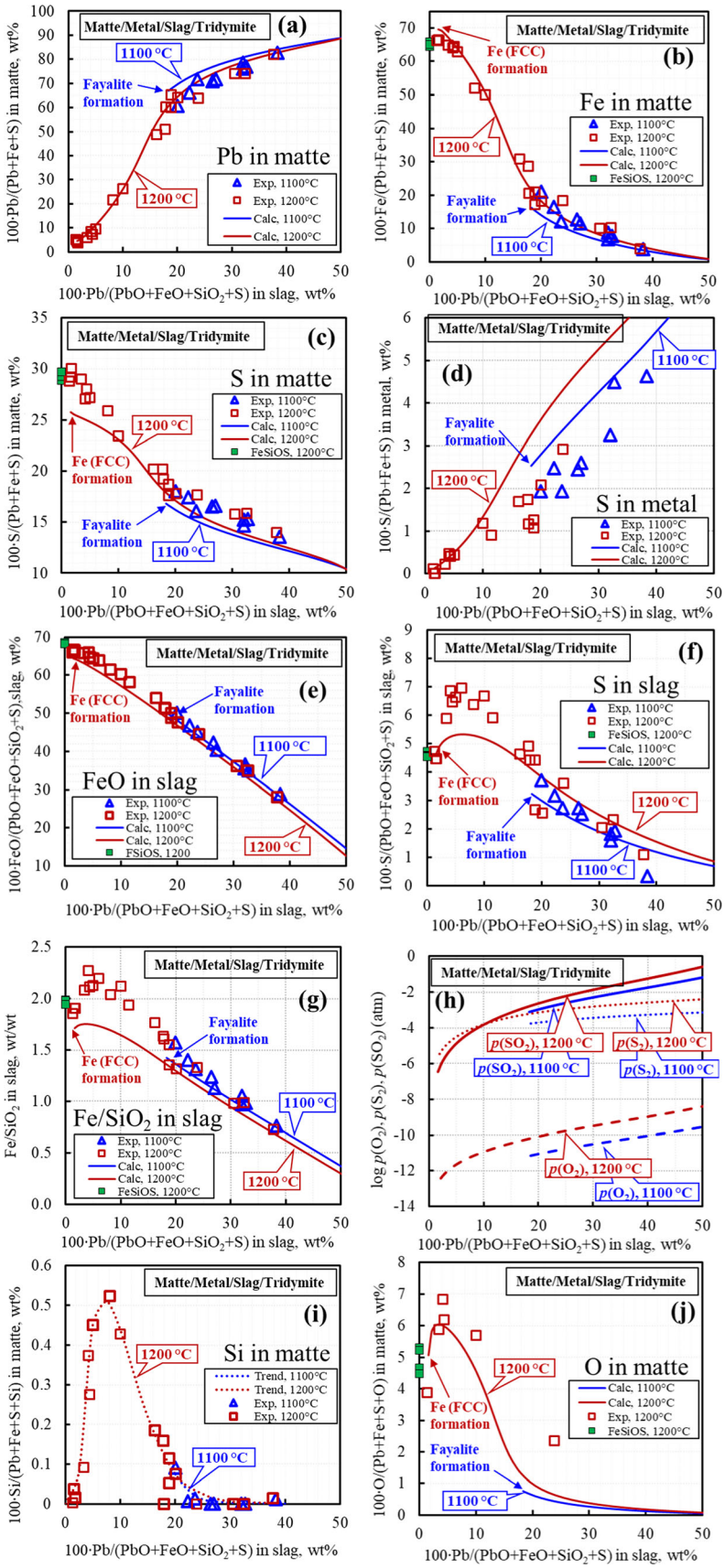
Matte/Metal/Slag/Tridymite
(a)
Pb in matte
Exp, 1100°C
Exp, 1200°C
Calc, 1100°C
Calc, 1200°C
1100 °C
1200 °C
Fayalite formation
100·Pb/(Pb+Fe+S) in matte, wt%
100·Pb/(PbO+FeO+SiO2+S) in slag, wt%
(b)
Fe in matte
FeSiOS, 1200°C
Fe (FCC) formation
100·Fe/(Pb+Fe+S) in matte, wt%
(c)
S in matte
100·S/(Pb+Fe+S) in matte, wt%
(d)
S in metal
100·S/(Pb+Fe+S) in metal, wt%
(e)
FeO in slag
FSiOS, 1200
100·FeO/(PbO+FeO+SiO2+S),slag, wt%
(f)
S in slag
100·S/(PbO+FeO+SiO2+S) in slag, wt%
(g)
Fe/SiO2 in slag
Fe/SiO2 in slag, wt/wt
(h)
p(SO2), 1200 °C
p(SO2), 1100 °C
p(S2), 1200 °C
p(S2), 1100 °C
p(O2), 1200 °C
p(O2), 1100 °C
log p(O2), p(S2), p(SO2) (atm)
(i)
Si in matte
Trend, 1100°C
Trend, 1200°C
100·Si/(Pb+Fe+S+Si) in matte, wt%
(j)
O in matte
Calc, 1100°C
Calc, 1200°C
Exp, 1200°C
FeSiOS, 1200°C
100·O/(Pb+Fe+S+O) in matte, wt%

◀Fig. 4—Experimental and thermodynamic modeling results for equilibria in the closed system, slag-matte-Pb metal-tridymite containing Pb-Fe-O-S-Si at 1100 °C and 1200 °C; (*a*) wt percent Pb in matte, (*b*) wt percent Fe in matte, (*c*) wt percent S in matte, (*d*) wt percent S in metal, (*e*) wt percent FeO in slag, (*f*) wt percent S in slag, (*g*) Fe/SiO_2 in slag, (*h*) $p(O_2)$, $p(S_2)$, and $p(SO_2)$, (*i*) wt percent Si in matte, (*j*) wt percent O in matte vs wt percent Pb in slag. The data marked "FeSiOS" are from Cu-free points in the study of the Cu-Fe-Si-O-S system.[51]

Taskinen[20] could not be used in the present study because the matte phase in that study was treated as a solution of stoichiometric FeS and PbS. Such model does not allow to resolve the inconsistency in experimental results on the eutectic temperature, and does not reproduce the deviation of matte towards excess metal as shown in Figure 3(a). Experimental results by Johto and Taskinen[20] were given less weigh because of the use of SEM–EDS for the measurement of composition. The characteristic S K-lines and Pb M-lines overlap can only be resolved using EPMA with special attention to peak separation.

The parameters for the Pb-O system were optimized to describe the experimental data assessed by Risold *et al.* [26]. The miscibility gap between metal and slag phase, enthalpy and temperature of melting of PbO, solubility of oxygen and $p(O_2)$ in the liquid Pb metal were reproduced. Deviation of oxide liquid towards excess metal up to 49 mol. pct O/(Pb + O) could not be reproduced by the model of the present study because separate solutions for slag and matte/metal phases were used. The generalized model describing slag/matte/metal as one solution with miscibility gaps is not practical, which was discussed in the assessment of the Cu-Fe-O-S-Si system.[10]

Originally, the $g^{10}_{Fe^{2+}Pb^{2+}/S^{2-}S^{2-}}$ and $g^{10}_{Fe^{3+}Pb^{2+}/S^{2-}S^{2-}}$ parameters in slag were introduced to better describe the distribution of minor concentrations of Pb between slag and matte in the Cu-Fe-O-S-Si-(Pb) system, as reported earlier.[50,51] Multi-component experimental data from the present study revealed some discrepancy for the distribution of lead in the Pb-Fe-O-S-Si system and those parameters were re-optimized. Moreover, the g°_{PbS} and $g^{001}_{Si^{4+}Pb^{2+}/O^{2-}O^{2-}(S^{2-})}$ in slag had to be introduced for completeness of the model for the slag. The lack of data was revealed to fix the values of these model parameters, which prompted an experimental study in the Pb-O-S-Si system.[12] The re-assessment of model parameters then followed, which included the data from previous studies[12,50,51] and the present study, with final values reported in Table IV. The final function g°_{PbS} in slag is selected to have similar heat capacity and entropy as Matte/metal solution phase at the composition of 1 mol Pb + 1 mol S and temperatures 1000–1200 °C, but the enthalpy is adjusted to more positive values, which describes the experimental data on solubility of sulfur in the PbO-SiO_2 slag and prevents the conflict with the Matte/metal phase. The parameter $g^{001}_{Si^{4+}Fe^{2+}/O^{2-}O^{2-}(S^{2-})}$ is proven to be more effective in describing the shape of the solubility of sulfur in PbO-SiO_2 slags,[12] compared to reciprocal parameter $g^{\circ}_{Si^{4+}Pb^{2+}/O^{2-}S^{2-}}$, and consistent with parameters $g^{101}_{Si^{4+}Fe^{2+}/O^{2-}O^{2-}(S^{2-})}$, $g^{101}_{Si^{4+}Ca^{2+}/O^{2-}O^{2-}(S^{2-})}$, and $g^{001}_{Si^{4+}Mg^{2+}/O^{2-}O^{2-}(S^{2-})}$ from earlier slag-matte studies.[10] The areas where quantitative description of experimental results was not achieved, even with refined model parameters are indicated below.

IV. DISCUSSIONS

A. *Closed Slag-Matte-Pb Metal-Tridymite Pb-Fe-O-S-Si System*

Comparison of the experimental measurements and thermodynamic modeling for the closed slag-matte-Pb metal-tridymite equilibria in the Pb-Fe-O-S-Si system at 1100 °C and 1200 °C is presented in Figures 4(a) through (j) as a function of the wt percent Pb concentration in the slag phase. For this condensed phase equilibria, it can be seen (Figure 4(a)) that the Pb concentration in the matte increases with increasing Pb concentration in the slag phase. The minimum of Pb in slag and matte at 1200 °C corresponds to the invariant slag-matte-Pb liquid metal-Fe solid metal-tridymite equilibrium. Three samples represent this point with the difference in the phase compositions within experimental uncertainty.

The concentration of lead in matte approaches the limiting value of 86.6 wt pct Pb (for pure PbS) at approximately 50 wt pct Pb in slag, where matte and metal merge into a single phase. The Pb distributes preferentially to the matte phase, however, the increase in Pb grade in matte is not linear with wt percent Pb in slag, particularly at high-Pb concentrations in matte. Since these mattes are close to the PbS-FeS join, the trends in wt percent Fe concentrations in matte (Figure 4(b)) are opposite to the wt percent Pb concentrations in matte. The wt percent S in matte (Figure 4(c)) decreases with increasing wt percent Pb in matte and wt percent Pb in slag. The solubility of S in Pb metal (Figure 4(d)) is significant. The solubility of S increases approximately linearly with wt percent PbO in slag and reaches to 5 wt pct at PbO = 40 wt pct, then the metal and matte eventually merge into one phase. Both the wt percent FeO (Figure 4(e)) and wt percent S (Figure 4(f)) in slag decrease approximately linearly with increasing wt percent Pb in slag. There are maxima of 7 pct S in slag and of Fe/SiO_2 = 2.2 in slag at approximately 6 wt pct Pb in slag, confirmed by repeated experiments. The current model describes the trend, but further work is needed to achieve better quantitative description of this region.

Silicon in matte reaches detectable levels (up to 0.5 wt pct) in the same range of compositions (5–15 wt pct Pb in slag) with the highest Fe/SiO_2 ratio and wt percent S in slag. Also, a maximum of oxygen in matte is observed in the same range. This trend is consistent with the tendency of the slag and matte to merge into single oxysulfide phase when approaching the FeS-FeO[8,11] join. Silicon has not been included into the current thermodynamic model of the matte phase; silicon in

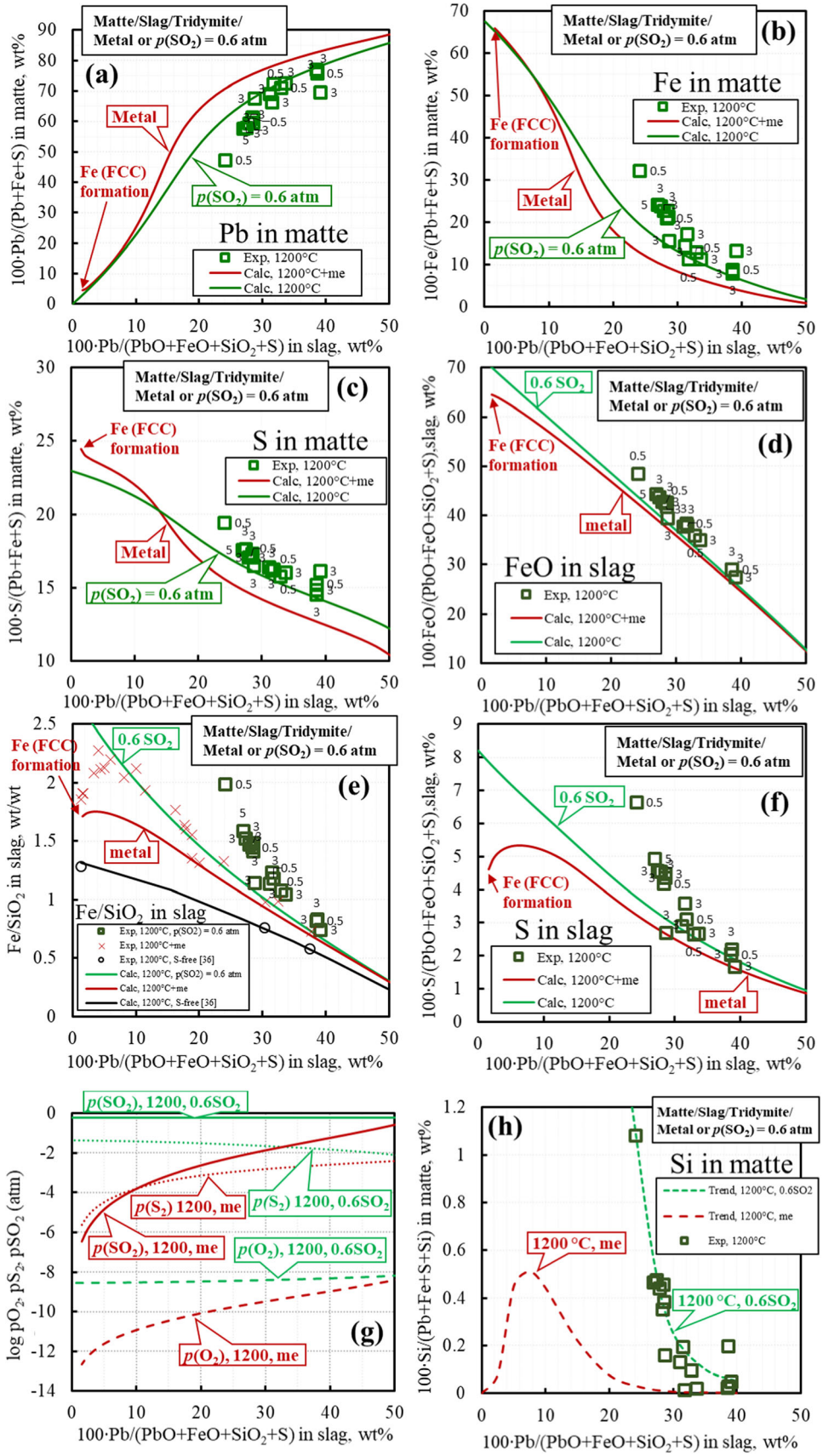
Matte/Slag/Tridymite/
Metal or $p(SO_2)$ = 0.6 atm
(a)
Metal
Fe (FCC) formation
$p(SO_2)$ = 0.6 atm
Pb in matte
Exp, 1200°C
Calc, 1200°C+me
Calc, 1200°C
100·Pb/(Pb+Fe+S) in matte, wt%
100·Pb/(PbO+FeO+SiO2+S) in slag, wt%
(b)
Fe in matte
100·Fe/(Pb+Fe+S) in matte, wt%
(c)
S in matte
100·S/(Pb+Fe+S) in matte, wt%
(d)
0.6 SO2
metal
FeO in slag
100·FeO/(PbO+FeO+SiO2+S),slag, wt%
(e)
Fe/SiO2 in slag
Exp, 1200°C, p(SO2) = 0.6 atm
Exp, 1200°C+me
Exp, 1200°C, S-free [36]
Calc, 1200°C, p(SO2) = 0.6 atm
Calc, 1200°C+me
Calc, 1200°C, S-free [36]
Fe/SiO2 in slag, wt/wt
(f)
S in slag
100·S/(PbO+FeO+SiO2+S),slag, wt%
(g)
p(SO2), 1200, 0.6SO2
p(S2) 1200, me
p(S2) 1200, 0.6SO2
p(SO2), 1200, me
p(O2), 1200, 0.6SO2
p(O2), 1200, me
log pO2, pS2, pSO2 (atm)
(h)
Si in matte
Trend, 1200°C, 0.6SO2
Trend, 1200°C, me
Exp, 1200°C
1200 °C, me
1200 °C, 0.6SO2
100·Si/(Pb+Fe+S+Si) in matte, wt%

◀Fig. 5—Experimental and thermodynamic modeling results for the semi-open, gas-slag-matte-tridymite equilibria in the Pb-Fe-O-S-Si system at 1200 °C and $p(SO_2)$ = 0.6 atm, (*a*) wt percent Pb in matte; (*b*) wt percent Fe in matte, (*c*) wt percent S in matte, (*d*) wt percent FeO in slag, (*e*) Fe/SiO_2 in slag,[37] (*f*) wt percent S in slag, (*g*) $p(O_2)$, $p(S_2)$, and $p(SO_2)$, (*h*) wt percent Si in matte vs wt percent Pb in slag. The labels near the points indicate equilibration time (hours). "me" in the legend means the presence of metal phase.

matte is not calculated and the line for Si in matte in Figure 4(i) is the experimental trend line. In all cases, the measured values at 1100 °C and 1200 °C are close, the differences determined experimentally are found to be close to the experimental uncertainty. The slag is stable in the range down to the minimum Pb concentration of 20 wt pct at 1100 °C, where Fe_2SiO_4 (fayalite) solid is formed. The sample containing slag, matte, metal, tridymite, and fayalite corresponds to this invariant equilibrium at 1100 °C. The oxygen, sulfur and sulfur dioxide partial pressure trends corresponding to the slag-matte-metal-tridymite equilibrium conditions predicted with the developed thermodynamic database are given in Figure 4(h). The oxygen and sulfur partial pressures increase by approximately two orders of magnitude and one order of magnitude, respectively, as Pb concentration in slag increases from 10 to 40 wt pct Pb. The trends in the Pb and Fe concentrations in matte and slag are well described by the current database, however, the current model underestimates the sulfur concentration in matte and slag. Some of the measured sulfur concentrations in the metal phase are lower than the model predictions due to difficulties in quenching the high-Pb metal phase that may partially segregate with the formation of matte. Further studies are needed to resolve experimental and thermodynamic modeling uncertainties.

B. *Semi-Open Gas-Slag-Matte-Tridymite Pb-Fe-O-S-Si System*

Comparison of the experimental measurements and thermodynamic modeling for the semi-open gas-slag-matte-tridymite equilibria in the Pb-Fe-O-S-Si system at 1200 °C and $p(SO_2)$ = 0.6 atm is presented in Figures 5(a) through (h). The labels near the points indicate equilibration time (hours). There is no significant difference between the compositions of the phases in the samples with equilibration times of 0.5 and 5 h. The curves obtained in equilibrium with Pb metal are included in the figures for comparison. It can be seen that the trends at $p(SO_2)$ = 0.6 atm closely follow those in equilibrium with metal, however, the absolute values are noticeably different from those obtained in equilibrium with metal. The concentrations of Pb and Fe in the matte phase are lower and higher, respectively, compared to those in equilibrium with metal for the same Pb in slag. The concentrations of S in the matte and slag phases at $p(SO_2)$ = 0.6 atm are higher than in equilibrium with metal. The increase in sulfur concentration in matte and slag at $p(SO_2)$ = 0.6 atm compared to equilibrium metal are consistent with model predictions. There is also an increase in Si solubility in matte compared to the lower $p(SO_2)$ for equilibrium with metal.

According to the experiments, a sharp increase in the mutual solubility between matte and slag is observed near Pb in slag around 10 wt pct. For instance, Figure 5(e) shows the increase in the Fe/SiO_2 ratio as a result of increasing $p(SO_2)$, which indicates higher mutual solubility. The results of the present study are compared with the S-free slag-metal-SiO_2(tridymite) equilibria in the Pb-Fe-O-Si system reported earlier.[37] Other indications are maximum of the concentration of sulfur in slag (Figure 5(f)), increased oxygen and silicon concentrations in matte (Figures 5(h), 4(j)). The model underestimates this effect, due the concept of separate solution models for the slag and matte phases. It is the limitation of the model, but in industrial applications, the presence of CaO, Al_2O_3 in slags, as well as Cu in mattes stabilizes the miscibility gap between slags and mattes, so better description is expected.

V. CONCLUSIONS

An integrated experimental and thermodynamic modeling approach has been used to determine and to quantitatively describe the chemical equilibria for the slag-matte-Pb metal-tridymite and gas-slag-matte-tridymite phase assemblages for the system Pb-Fe-O-S-Si. The experimental measurements include concentrations of each of these elements present in the respective phases in equilibrium. The experimental data obtained for the slag-matte-metal-tridymite phase equilibria at 1100 and 1200 °C are reported; the slags containing up to approximately 40 wt pct PbO have been investigated. The results indicated that the change of temperature from 1200 °C to 1100 °C had relatively small effect on the slag-matte-metal-tridymite equilibria. The Pb distributes preferentially into the matte phase over the slag phase for all compositions studied. Sulfur dissolved in metal increases with increasing wt percent Pb in slag because the miscibility gap between matte and metal closes at higher concentration of Pb in the system. Measurements have also been undertaken for the gas-slag-matte-tridymite equilibria at $p(SO_2)$ = 0.6 atm at 1200 °C for slags containing between 20 and 40 wt pct PbO. The effective sulfur pressures and oxygen partial pressures ($p(O_2) \approx 10^{-8}$ atm) were higher than in equilibrium with metal for the range of compositions investigated. The results showed higher concentration of iron in matte and sulfur in slag for these high $p(SO_2)$ conditions, relative to equilibrium with metal. Present results are the first systematic quantitative experimental data on phase compositions in equilibrium in this Pb-Fe-O-S-Si system. The thermodynamic model describes the observed trends in experimental data and can now be used for predictions. Quantitative differences were identified. The main reason for the deviation of the model from the experiments resulting in tendencies of slag and matte to form a single oxysulfide solutions, which are not well predicted using separate

solutions for the slag and matte. These differences are expected to be less significant in practical applications, where the presence of CaO, Al_2O_3, and Cu stabilizes the miscibility gap between slag and matte. Results are particularly important for further development of the multi-component thermodynamic database and eventually—for the optimization of industrial operations and development of new processes.

ACKNOWLEDGMENTS

The authors would like to thank Australian Research Council Linkage Program LP180100028, Aurubis (Germany), Boliden (Swidden), Kazzinc Glencore (Kazakhstan), Nyrstar (Australia), Outotec Oy (Espoo) (Finland), Penoles (Mexico), and Umicore (Belgium) for the financial and technical support for this study. The authors would like to also thank the staff of the Centre for Microscopy and Microanalysis, University of Queensland for their technical support.

CONFLICT OF INTEREST

On behalf of all authors, the corresponding author states that there is no conflict of interest.

FUNDING

Open Access funding enabled and organized by CAUL and its Member Institutions.

OPEN ACCESS

REFERENCES

1. A. Siegmund: *Metall. Mater. Process.: Princ. Technol., Yazawa Int. Symp.*, F. Kongoli, ed., Minerals, Metals & Materials Society, Warrendale, PA, 2003, pp. 43-62.
2. N. Dosmukhamedov and V. Kaplan: *JOM*, 2017, vol. 69(2), pp. 381-87.
3. B. Blanpain, S. Arnout, M. Chintinne, and D.R. Swinbourne: *Handbook of Recycling*, E. Worrell, and M. Reuter, eds., 2014, pp. 95-111.
4. C. Zschiesche, and I. Bauer: *9th International Symposium on Lead and Zinc Processing*, San Diego, USA, Springer, Cham, 2020, pp. 739-57.
5. T. Rytkonen and A. Taskinen: *Scand. J. Metall.*, 1986, vol. 15(1), pp. 25-29.
6. L. Fontainas, M. Coussement and R. Maes: *Complex Metall. '78, Pap. Int. Symp*, 1978, pp. 13-23.
7. S. Amout, E. Nagels, and B. Blanpain: *European Metallurgical Conference*, Duesseldorf, Germany, GDMB Informations GmbH, Clausthal-Zellerfeld, 2011, pp. 363-72.
8. A. Yazawa and M. Kameda: *Technol. Rep. Tohoku Univ.*, 1953, vol. 18(1), pp. 40-58.
9. Y. Takeda: *5th Int. Conf. Molten Slags, Fluxes Salts*, Iron and Steel Society Warrendale, PA, 1997, pp. 735-43.
10. D. Shishin, S.A. Decterov, and E. Jak: *J. Phase Equilib. Diffus.*, 2018, vol. 39(5), pp. 456-75.
11. Y. Jo, H.-G. Lee, and Y.-B. Kang: *ISIJ Int.*, 2013, vol. 53(5), pp. 751-60.
12. D. Shishin, M. Shevchenko, V. Prostakova, P.C. Hayes, and E. Jak: *11th International Conference on Molten Slags, Fluxes and Salts*, Seoul, Korea, E-proceedings, 2021, pp. EA20191129–0862.
13. V.D. Chaskar: *The Solubility of Lead in Iron Suflide and Oxisulfide Mattes at 1100 Degrees and 1200 Degrees*, Ph.D. thesis, University of Missouri-Rolla, Rolla, MO, 1976.
14. H.R. Eric and H. Ozok: *Metall. Mater. Trans. B*, 1994, vol. 25, pp. 53-61.
15. V. Gontarev: Master's thesis, University of Ljubljana, Ljubljana, 1976.
16. R.C. Kerby: Canadian Mines Bureau of Investigation Report No. IR 73–49, Department of Energy, Mines and Resources, Ottawa, 1973, pp. 18.
17. R. Brett and G. Kullerud: *Econ. Geol.*, 1967, vol. 62(3), pp. 354-69.
18. K.K. Avetisyan and G.I. Gnatyshenko: *Izv. Akad. Nauk. Kaz. SSR Ser. Gorn. Dela Met. Stroit. Stroim.*, 1956, vol. 6, pp. 11-25.
19. K. Friedrich: *Metallurgie*, 1907, vol. 4, pp. 479-85.
20. H. Johto and P. Taskinen: *Eur. Metall. Conf. Duesseldorf, Germany*, 2011, vol. 4, pp. 1127-36.
21. J.E. Dutrizac: *Can. J. Chem.*, 1980, vol. 58(7), pp. 739-43.
22. S.A. Decterov and A.D. Pelton: *Metall. Mater. Trans. B*, 1999, vol. 30B(6), pp. 1033-44.
23. E. Jak, P.C. Hayes, and H.-G. Lee: *Korean J. Miner. Mater. Inst. (Seoul)*, 1995, vol. 1(1), pp. 1-8.
24. E. Jak: *9th Intl. Conf. on Molten Slags, Fluxes and Salts*, Beijing, China, The Chinese Society for Metals, 2012, pp. 1-28, w77.
25. T. Hidayat, A. Fallah Mehrjardi, M. Shevchenko, P.C. Hayes and E. Jak: unpublished research, University of Queensland, Brisbane, Australia, 2020, Submitted to Metall. Mater. Trans. B.
26. D. Risold, J.-I. Nagata, and R.O. Suzuki: *J. Phase Equilib*, 1998, vol. 19(3), pp. 213-33.
27. A. Fallah-Mehrjardi, T. Hidayat, P.C. Hayes, and E. Jak: *Metall. Mater. Trans. B*, 2017, vol. 48(6), pp. 3002-16.
28. S. Sineva, M. Shevchenko, P.C. Hayes, and E. Jak: *Miner. Process. Extr. Metall. Rev.*, 2021, https://doi.org/10.1080/08827508.2021.1998042.
29. M. Shevchenko and E. Jak: *Metall. Mater. Trans. B*, 2018, vol. 49(1), pp. 159-80.
30. M. Shevchenko and E. Jak: *J. Phase Equilib. Diffus.*, 2019, vol. 40(2), pp. 128-37.
31. M. Shevchenko and E. Jak: *J. Phase Equilib. Diffus.*, 2019, vol. 40(5), pp. 671-85.
32. E. Jak, M. Shevchenko, D. Shishin, T. Hidayat, and P.C. Hayes: *9th International Symposium on Lead and Zinc Processing*, San Diego, USA, Springer, Cham, 2020, pp. 337–349.
33. D. Shishin, P.C. Hayes, E. Jak: *58th Annual Conference of Metallurgists Copper 2019*, Vancouver, Canada, MetSoc, 2019, p. 594861.
34. T. Hidayat and E. Jak: *Int. J. Mater. Res.*, 2014, vol. 105(3), pp. 249-57.
35. T. Hidayat, D. Shishin, S.A. Decterov, and E. Jak: *J. Phase Equilib. Diffus.*, 2017, vol. 38(4), pp. 477-92.

36. T. Hidayat, D. Shishin, S. Decterov, and E. Jak: *Calphad*, 2017, vol. 58, pp. 101-14.
37. M. Shevchenko and E. Jak: *Calphad*, 2019, vol. 67, p. 101670.
38. T. Hidayat, D. Shishin, E. Jak, and S. Decterov: *Calphad*, 2015, vol. 48, pp. 131-44.
39. P. Waldner and A.D. Pelton: *J. Phase Equilib. Diffus.*, 2005, vol. 26, pp. 23-28.
40. P. Waldner, and A.D. Pelton: *Thermodynamic Modeling of the Cu-Fe-S System, Ecole Polytechnique de Montreal*, Internal report, Montreal, QC, Canada, 2006.
41. D. Shishin, *Development of a Thermodynamic Database for Copper Smelting and Converting*, Ph. D. thesis, Ecole Polytechnique of Montreal, 2013.
42. D. Shishin and S.A. Decterov: *Calphad*, 2012, vol. 38, pp. 59-70.
43. D. Shishin, T. Hidayat, E. Jak, and S. Decterov: *Calphad*, 2013, vol. 41, pp. 160-79.
44. D. Shishin, E. Jak, and S.A. Decterov: *J. Phase Equilib. Diffus.*, 2015, vol. 36(3), pp. 224-40.
45. D. Shishin, E. Jak, and S.A. Decterov: *Calphad*, 2015, vol. 50, pp. 144-60.
46. D. Shishin, J. Chen, and E. Jak: *J. Phase Equilib. Diffus.*, 2020, vol. 41(3), pp. 218-33.
47. D. Shishin, T. Hidayat, U. Sultana, M. Shevchenko, and E. Jak: *Int. J. Mater. Res.*, 2020, vol. 111(9), pp. 733-43.
48. I. Vaajamo and P. Taskinen: *Thermochim. Acta*, 2011, vol. 524(1), pp. 56-61.
49. G. Eriksson and A.D. Pelton: *Metall. Trans.*, 1993, vol. 24, pp. 807-16.
50. T. Hidayat, J. Chen, P.C. Hayes, and E. Jak: *Metall. Mater. Trans. B*, 2019, vol. 50, pp. 229-41.
51. S. Sineva, M. Shevchenko, P.C. Hayes, and E. Jak: *Miner. Process. Extr. Metall. Rev.*, 2022, vol. 43(8), pp. 989-99.